A Power Scaling Strategy for Longitudinally Diode-Pumped Tm:YLF Lasers

S. So[1], J.I. Mackenzie[1], D.P. Shepherd[1], W.A. Clarkson[1], J.G. Betterton[2] and E.K. Gorton[2]

[1]Optoelectronics Research Centre

University of Southampton, Highfield, Southampton SO17 IBJ, U.K.

Fax: +44 (0)23 80593142, Email: dps@orc.soton.ac.uk

[2]QinetiQ

St. Andrews Road, Malvern, Worcestershire WR14 3PS, U.K.

Abstract

We describe a power scaling strategy for longitudinally diode-pumped Tm:YLF lasers based on optimisation of the thulium doping level and the gain geometry. Carefully designed laser experiments at lower powers are shown to allow a simple means for accurately predicting the thermal loading and hence the power scaling properties of this system, including the effects of ground-state depletion, cross-relaxation and energy transfer upconversion. An optimised doping level of 2at.% and a slab geometry are shown experimentally to allow scaling of a single gain unit to output powers of ~70W, limited by the available pump power, and a strategy for scaling well beyond 100W output is discussed.

PACS: 42.55.-f Lasers; 42.55.Xi Diode Pumped Lasers; 42.60.By Design of specific Laser Systems.

1 Introduction

Two-micron thulium and thulium-pumped-holmium laser sources are of interest for many applications in the scientific, defence, and medical fields. Thulium has a strong and broad absorption band at ~800nm that is ideal for diode pumping [1] and benefits from an efficiency-enhancing cross-relaxation process that can lead to two ions in the upper laser level for one pump photon. Thulium readily substitutes into many crystal hosts that are suitable for high-average-power laser systems, but YLF is a particularly attractive choice as the host medium when it is used as a pump source for a 2.1µm Ho:YAG laser [1]. This is due to the good overlap of its emission peaks with the absorption spectrum of Ho:YAG. YLF is also attractive due to the fact that it has a decrease in refractive index with temperature, leading to a negative thermal lens that is partly offset by a positive lensing effect caused by bulging of the end-faces. Thus the overall thermal lensing effect is very weak, especially for the σ-polarised emission at 1.9µm. Furthermore, YLF is a naturally birefringent material, capable of producing linearly polarised output with virtually no depolarisation loss. Due to these attractive features thulium-doped YLF has been investigated by previous workers, with several tens of Watts being reported in end-, [1,2], and side-pumped configurations, [3], respectively. However, average output powers from single laser gain components have so far been limited to ~20W. This was in part due to the limited available diode pump power, but was also due to the low thermal stress fracture limit for YLF, [4]. In this work we describe a strategy for power scaling diode-end-pumped single Tm:YLF gain components towards the 100W regime, based on the optimisation of the thulium doping level and the geometry of the gain medium. The development of this strategy is based upon studies of carefully designed laser performance experiments that automatically contain information about all the

competing heat-deposition processes, mostly avoiding the need for separate and potentially complicated spectroscopic measurements of the transition rates for each process.

2 Doping Level

Normally, one might expect that using a low doping level and a longer absorption length for the pump, within the stringent limits set by the brightness of high-power diode pump sources, would be beneficial for overcoming thermal effects, as less heat would be deposited per unit length from the quantum defect between the pump and laser photon energies. Indeed, this strategy has been successfully employed in end-pumped Nd:YLF, [5], where it also benefits from reduced upconversion effects. However, in thulium the choice of doping level depends upon a balance of counteracting effects, as shown in the schematic energy level diagram of figure 1. As with Nd:YLF, a low doping concentration leads to less heat deposited (via non-radiative decay) per unit length due to weaker pump absorption and reduced energy transfer upconversion (ETU). However, a low doping level also reduces the cross-relaxation process, reducing the number of ions excited to the upper laser level per pump photon (quantum yield), and thus increasing the heat deposited per unit length. Consequently, one must find an optimum doping level that balances these effects, which we define as the doping level that leads to maximum output power before thermal stress fracture occurs.

The performance of a Tm:YLF laser will be affected by the cross-relaxation and ETU processes in different ways. Increasing the quantum yield (*QY*) leads to both a decrease in threshold and an increase in slope efficiency. However, ETU can be thought of as effectively reducing the lifetime of the upper laser level, [6], and

consequently it affects the threshold but not the slope efficiency of the laser, [7]. This argument is based upon a plane-wave analysis and it should be noted that if transverse spatial profiles are taken into account then it is possible for ETU to have an effect on the slope efficiency. In our case the large uniform pumping inversion will initially be more strongly depleted at the centre by the smaller lasing mode, causing a reduction in ETU in this region compared to the edges. Numerical simulations accounting for such spatial profiles show that the effect on slope efficiency is typically very small and negligible when well above threshold. Thus it is possible in carefully designed laser experiments to separate cross-relaxation and ETU effects, and with experimental evidence of the point at which fracture occurs, a prediction for the optimum doping level and the output powers achievable is allowed.

3 Laser Performance of End-Pumped Tm:YLF Rods

Three Tm:YLF rods of 2, 4 and 6at.% Tm doping level were set up in laser cavities such that, in the absence of cross-relaxation and ETU processes, their threshold should be the same. In order to achieve this goal, the rod lengths were chosen to each correspond to two pump absorption lengths (24, 12 and 8mm, respectively), keeping approximately constant pump, w_p , and laser, w_l , mode sizes, and ensuring that $w_p >> w_l$. The latter condition leads to multi-transverse mode operation with a constant pump/signal spatial overlap, and minimises the effects of thermally induced aberrations on the laser performance [8].

The 3mm diameter (a-cut) Tm:YLF laser rods had antireflection coated end-faces for the pump and lasing wavelengths of 792nm and ~1.9µm respectively. All rods were mounted in water-cooled copper blocks, held at 18^{o}C, to allow effective

heat removal and were pumped by a high-power diode pump source at 792nm. The latter consisted of two low fill-factor water-cooled diode bars, collimated in the fast and slow-axes with micro-lenses, and polarisation combined to produce a single beam. A two-mirror beam-shaper, [9], was employed to re-format the beam with roughly equal beam quality factors in orthogonal planes resulting in values of $M_x^2 \approx 80$ (parallel to the array) and $M_y^2 \approx 52$ (perpendicular to the array) and a maximum power of 52W. A uniform and quasi-top-hat pump distribution was desirable for the comparative studies, hence the output beam from the pump source was 'homogenised' by coupling into a multi-mode fibre with a core diameter of 365μm and NA of 0.22. A spatial filter was then employed to reduce the M^2 value to 100 allowing relatively tight pump focussing with minimal diffraction spreading even in the longest Tm:YLF rod under investigation, but limiting the maximum available pump power to 33W.

A simple two-mirror resonator configuration was employed, comprising a plane pump in-coupling mirror with high reflectivity at the lasing wavelength and high transmission at the pump wavelength, and an 87% reflectivity concave output coupler with a radius of curvature of 200mm. A cavity length of 100-120mm was selected to produce a calculated TEM_{oo} beam waist ($1/e^2$ radius of intensity) in the YLF crystal (under un-pumped conditions) of 260μm, which was predicted to increase by up to 50% at the maximum available pump power due to the effect of the weak negative thermal lensing in Tm:YLF. The pump beam was focussed to a waist of $w_p \approx 470\mu m$, roughly equal to that required for confocal pumping of the longest rod (i.e. $w_p=(M^2\lambda_p L/2n\pi)^{1/2}$), and positioned at the mid-point of each laser rod respectively. All three crystals were then characterised through their threshold and slope efficiency with the results shown in figure 2. In all the following results slope

efficiencies are measured for data points greater than 3 times threshold in order to remove the effect of the well-know quasi-three-level laser behaviour of reduced slope efficiency near threshold.

From figure 2 we note that the slope efficiency for the 2 at.% doped rod is 0.89 times lower than that for the 4at.% rod, which we attribute to a lower *QY*. An estimation of *QY* as a function of doping concentration can been calculated, see figure 3, following the method of Honea *et. al.*, [10], where the reported Tm:YLF lifetime measurements for various doping concentrations by Armagan *et. al.*, [11], and the $^3H_4 \rightarrow {}^3F_4$ branching ratio after Walsh *et. al.*,. [12], have been used. An excellent agreement is found when comparing the ratio of the predicted *QY* values for 2 and 4at.% Tm (0.88) with that from the measured slope efficiencies (0.89). It should also be noted that the 53% slope efficiency is much greater than the maximum possible in the absence of cross-relaxation (41%) and that the relatively small increase in slope efficiency from doubling the Tm concentration from 2 to 4at% is indicative of being in the nearly saturated $QY \approx 2$ regime. We are therefore confident in using the theoretical *QY* versus doping level values in further power scaling calculations.

The results of figure 2 also show a very small decrease in threshold from 5.9W to 5.6W in going from 2 to 4 at.% Tm doping, which is mostly accounted for by the change in *QY*, suggesting that ETU effects are small in this regime, and at this point we assume that it is zero for 2at.%. However, rather than a lower threshold due to a higher *QY*, we find that the 6at.% rod had a significantly higher threshold and indeed fractures at just 17W of absorbed power. The observed threshold of 8.0W is 2.9W higher than we would expect from scaling the observed threshold from the 2at.% rod

solely accounting for the higher *QY*. This power difference, P_{ETU} , is attributed to ETU and is totally converted to heating the YLF crystal. It should be noted that this effective power loss is clamped at this threshold value as the inversion is also clamped at this point. This reasoning allows us to write down the following equation for the heat load above threshold, P_h , for a given absorbed pump power, P_{abs} , accounting for the quantum defect, cross relaxation, and ETU.

$$P_h = \left(1 - QY\frac{\lambda_p}{\lambda_s}\right)\left(P_{abs} - P_{ETU}\right) + P_{ETU} \qquad \ldots.(1)$$

The maximum stress, $\sigma_{\max}$, which YLF can tolerate in an end-pumped configuration before fracture occurs is dependent upon its material parameters, the pump beam size and the rod diameter [13]. The relevant variable parameters for comparison here are the absorption coefficient, α_{abs}, and the heat load, P_h:

$$\sigma_{\max} \propto \alpha_{abs} P_{h\_\max} \qquad \ldots(2)$$

We can now make the power scaling predictions shown in table 1 for various Tm doping levels in YLF. It should be noted that the experimental values for the absorption coefficient were taken at diode pump powers equivalent to lasing threshold, thus accounting for any depletion of the ground state population, which again will not change above threshold as the populations become clamped at this point. Table 1 predicts an optimum doping of 2at.%, lower than the 3at.% used by previous workers [1,2]. This is despite the fact that in table 1 we take the optimistic power scaling assumption that the ETU is still negligible at the 3at.% doping level.

Maximum output power limits of around 20W are predicted, in agreement with previous workers findings [1,2], who have used bonded end-caps and double-ended pumping to achieve 22W of output from a single Tm:YLF rod and 36W using two Tm:YLF rods. It should be noted that the prediction for output powers used effective thresholds found from the slope efficiency fits shown in figure 2, or by scaling from them. A factor-of-two improvement should be available, according to theory, [13], if the pump nearly fills the rod aperture, but this is not sufficient to reach the 100W output power regime.

In order to gain some experimental verification of these power scaling predictions we increased the power of the pump source to allow us to reach the fracture point of the 4at% rod. This new pump source consisted of a 6-bar low-fill-factor diode stack, with each bar collimated in the fast and slow-axes with micro-lenses. The final beam-shaped diode stack beam-quality was $M_x^2 \approx 160$ and $M_y^2 \approx 100$ with a maximum power of 265W. To produce a similar beam-quality from the diode stacks as had been used previously, a spatial filtering slit was employed in the x-axis only, limiting the available incident power to 115W. With identical pump parameters and cavity configurations as used for the diode-bar pumping, the results shown in figure 4 were obtained. Once again the ratio of the slope efficiencies fitted 3 times above threshold (0.92) was in good agreement with that expected from the theoretical QY curve of figure 3 (0.88). Furthermore, the 4at.% rod fractured at an absorbed power of 38.5W and an output power of 14.5W, in good agreement with our scaling predictions of 38.7W and 15.9W, respectively. Thus we can conclude that the optimum doping level for power scaling Tm:YLF in an end-pumped continuous wave

laser is 2at.% and that if the gain medium has a rod geometry scaling much beyond 20W is problematic.

4 Gain Medium Geometry

It is well known that a uniformly pumped slab geometry, with its large cooling surfaces, benefits from an increase in its fracture limit when compared to a rod with the scaling law, [14],

$$\frac{P_{h\_\max}(slab)}{P_{h\_\max}(rod)} = \frac{3}{2\pi}\left(\frac{w}{t}\right) \qquad \ldots(3)$$

where *w* is the width of the slab and *t* is the thickness. The scaling law is not so clear for a non-uniformly pumped slab but from numerical modelling it has been shown that it still depends on the ratio of slab thickness to width of the pumped area, [15]. Noting that an improvement of approximately a factor of 5 would be required in order to get to the 100W output power regime, we can estimate that a slab aspect ratio of 10 to 1 is required.

5 Laser performance of End-Pumped Tm:YLF Slabs

The power scaling offered by the slab geometry was tested by using a 9mm-wide (c-axis) by 1.5mm-thick, 20mm-long 2at.% Tm-doped YLF gain element. The input face of the slab was AR coated at the pump and laser wavelength, and its output face was AR coated at the laser wavelength and had >90% reflectivity at the pump wavelength. As this slab has an aspect ratio of just 6, the simple scaling law of eqn.(3) would lead to an expected fracture point of 158W of absorbed pump power.

The slab was sandwiched between two water-cooled copper heat-sinks (water temperature 16^{o}C) using 0.1mm-thick indium foil.

In order to test the slab in this regime we used the same diode stack as was used in the high-power rod experiments except that it was not beam shaped or spatially filtered, and so delivered nearly 300W in a beam with measured M^2 values of 40 in the y-axis and 450 in the x-axis (the plane of the slab). The beam was demagnified with a cylindrical lens telescope to a collimated beam that nearly filled the slab in the x-axis ($1/e^2$ diameter of 8mm), and a further single cylindrical lens was used to confocally focus in the y-axis over a double pass of the YLF slab ($1/e^2$ waist diameter of 0.74mm located near the output face). This focussing arrangement avoided local pumping hot-spots, which can occur if the individual diode emitters are re-imaged within the YLF crystal. The resonator was formed by a plane high reflectivity input coupling mirror and a 200mm radius of curvature 87% reflectivity output coupler, with a cavity length of approximately 50mm. The lasing mode was observed to nearly fill the slab aperture with a super-Gaussian-like profile in the plane of the slab and an approximately Gaussian profile in the vertical axis, with corrsponding M^2 values of 350 and 3.5. Figure 5 shows the lasing performance obtained with this set-up. Firstly, we note that the lasing threshold of 47W agrees very well with a simple scaling of the 2at.% Tm:YLF rod results in accordance with the increased pump area. Additionally, the slope efficiency is only slightly lower than that obtained for the rods, possibly due to a slightly higher intracavity loss from the dual AR/HR coating used on the slab output face or from increased diffraction losses. Finally, we note that despite reaching absorbed powers of up to 218W and output powers of 68W, fracture was not observed. This better than predicted performance

may be due to somewhat better heat-sinking in the case of the slab compared to the rod, or indeed small variations in other parameters such as surface finish. It may also be due to the fact that our slabs are not uniformly pumped and so the exact nature of the scaling from the rod results is not clear. However, when a 2mm-thick slab was used in the same set-up, fracture was observed at an absorbed power level of 200W. If we scale from this figure to our current 1.5mm slab the expected fracture point is 267W of absorbed power and an output of 90W.

If we wished to scale to the 100W regime it seems that we would need a higher aspect ratio slab. One method of achieving this would be to go thinner than the current 1.5mm. However, for our pump beam quality (M_y^2=40) and the length set by the 2at.% optimum doping level (~20mm), we would quickly enter the pump guiding regime. This brings added complications as we would not be able to use simple contact with water-cooled heat-sinks without an intermediate lower index layer. One possibility would be to deposit MgF layers on the top and bottom surface. An alternative to a thinner slab is a wider slab but current commercially available YLF always has one of the a-axes limited to ~10mm in length. One solution here would be to use two slabs of similar dimensions to that used in this work, which would allow pumping into the 1.5mm by 20mm aperture and using the two 9mm length directions to achieve sufficient pump absorption. Simple scaling predictions for this two-slab system, for example by polarisation-combining two stacks to achieve sufficient pump power, leads to an expected effective threshold of 140W absorbed power, a fracture absorbed power limit of 593W, and thus a maximum output power of 199W (assuming the same 44% slope efficiency). Thus output power well beyond 100W is clearly feasible.

6 Conclusion

We have developed a power scaling strategy for taking the 2μm output of Tm:YLF lasers into the 100W regime. The strategy was based on scaling from carefully designed low-power laser experiments which automatically include the various competing heat-deposition effects occurring in this laser system. We find an optimum Tm doping level, for providing the maximum output power before thermally induced fracture occurs, of 2at.%. We also experimentally demonstrated the superiority of the slab geometry, allowing experimental demonstration of output powers up to nearly 70W from a single gain unit, limited by the available pump power. Scaling into the 100W regime and beyond is shown to require slabs with aspect ratios of ~10, which would require either a pump guiding geometry or, due to the current limitations on the size of commercially available Tm:YLF crystals, the use of two slabs. Our future work will aim to experimentally demonstrate output powers in this regime and investigate cavity designs to enable high-brightness output. Tm:YLF lasers at this power level are especially interesting for power scaling the output of 2.1μm Ho:YAG lasers.

ACKNOWLEDGEMENTS

The work was carried out under the auspices of the UK Ministry of Defence Corporate Research Programme. Sik So wishes to acknowledge the support of an EPSRC funded PhD studentship and Jacob Mackenzie acknowledges the support of a Royal Academy of Engineering post-doctoral fellowship.

REFERENCES

[1] P.A. Budni, M.L. Lemons, J.R. Mosto, E.P. Chicklis: IEEE J. Sel. Top. Quantum Electron. **6,** 629 (2000).

[2] L.A. Pomeranz, P.A. Budni, M.L. Lemons, C.A. Miller, J.R. Mosto, T.M.Pollak, E.P. Chicklis, in: OSA *Trends in Optics and Photonics, Vol. 26, Advanced Solid-State Lasers, M. Fejer, H. Injeyan and U. Keller, eds.* (Optical Society of Amerca, Washington, DC 1999), p.458.

[3] A. Dergachev, K. Wall, P.F. Moulton, in: OSA *Trends in Optics and Photonics, Vol. 68, Advanced Solid-State Lasers, M.E. Fermann and L.R. Marshall, eds.* (Optical Society of Amerca, Washington, DC 2002), p.343.

[4] D.C. Shannon, D.L. Vecht, S. Re, J. Alonis, R.W. Wallace: SPIE **1865**, 164 (1993).

[5] P.J. Hardman, W.A. Clarkson, G.J. Friel, M. Pollnau, D.C. Hanna: IEEE J. Quantum Electron. **35**, 647 (1999).

[6] J.I. Mackenzie, C. Li, D.P. Shepherd, R.J. Beach, S.C Mitchell: IEEE J. Quantum Electron. **38**, 222 (2002).

[7] G. Rustad, K. Stenersen: IEEE J. Quantum Electron. **32**, 1645 (1996).

[8] W.A. Clarkson: J. Phys. D: Appl. Phys. **34**, 2381 (2001).

[9] W.A. Clarkson, D.C. Hanna: Opt. Lett. **21**, 375 (1996)

[10] E.C. Honea, R.J. Beach, S.B. Sutton, J.A. Speth, S.C. Mitchell, J.A. Skidmore, M.A. Emanuel, S.A. Payne: IEEE J. Quantum Electron. **33**, 1592 (1997).

[11] G. Armagan, A.M. Buoncristiani, A.T. Inge, B.D. Bartolo: in *OSA Trends in Optics and Photonics, vol. 10, Advanced Solid-State Lasers,G. Dube and L.L. Chase, eds.* (Optical Society of America, Washington, DC 1991), p. 222.

[12] B.M. Walsh, N.P. Barnes, B. Di Bartolo: J. Appl. Phys. **83**, 2772 (1998).

[13] L. Yan, C.H. Lee: J. Appl. Phys. **75**, 1286 (1994).

[14] J.M. Eggleston, T.J. Kane, K. Khun, J. Unternahrer, R.L. Byer: IEEE J. Quantum Electron. **20**, 289 (1984).

[15] R. Paschotta, J. Aus der Au, U. Keller: IEEE J. Sel. Top. Quantum Electron. **6**, 636 (2000).

Figure Captions

Figure 1 Schematic energy level diagram of the various heat depositing effects in a 2µm thulium laser system.

Figure 2 Output power against absorbed power for diode-bar-pumped 2, 4 and 6 at.% Tm-doped YLF rods.

Figure 3 Theoretical calculation of quantum yield against Tm doping level for YLF.

Figure 4 Output power against absorbed power for diode-stack-pumped 2 and 4 at.% Tm-doped YLF rods.

Figure 5 Output power against absorbed power for a diode-stack-pumped 2at.% Tm-doped YLF slab.

Table Captions

Table 1 Tabulated Power Scaling Calculations. * indicates an experimental value. ** indicates assumed values for 3at.% leading to an optimistic power scaling. All other values are either theoretical or scaled from experimental values.

Table 1

Tm Doping Level / at.%	**1**	**2**	**3**	**4**	**6**
Quantum Yield	1.15	1.68	1.84	1.91	1.96
Slope Efficiency / %	32	47*	51	53	55
Absorption Coefficient / cm^{-1}	0.36	0.71*	1.07	1.43*	2.14*
Absorbed Power Threshold / W	7.9	5.9*	5.6**	5.6*	8.0*
Threshold in Absence of ETU / W	7.9	5.9	5.6**	5.2	5.1
P_{ETU} / W	0	0	0**	0.4	2.9
P_{h_max} / W	33.0	16.5	11.0	8.2	5.5*
Maximum Absorbed Power / W	63.4	55.1	47.2	38.7	17.0*
Effective Threshold / W	13.4	9.2*	8.4	8.7*	-
Maximum Output Power /W	16.0	21.6	19.8	15.9	2.5*

Figure 1.

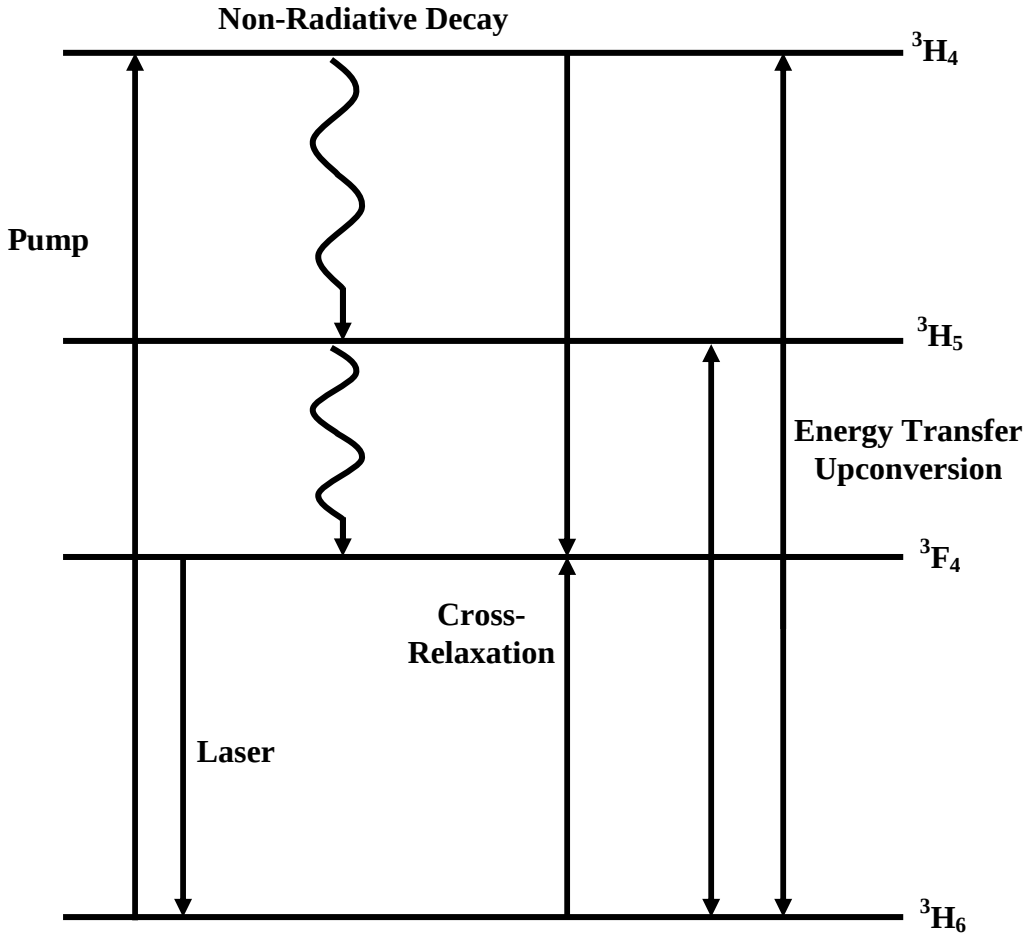
Non-Radiative Decay
$^3H_4$
Pump
$^3H_5$
Energy Transfer
Upconversion
$^3F_4$
Cross-
Relaxation
Laser
$^3H_6$

Figure 2

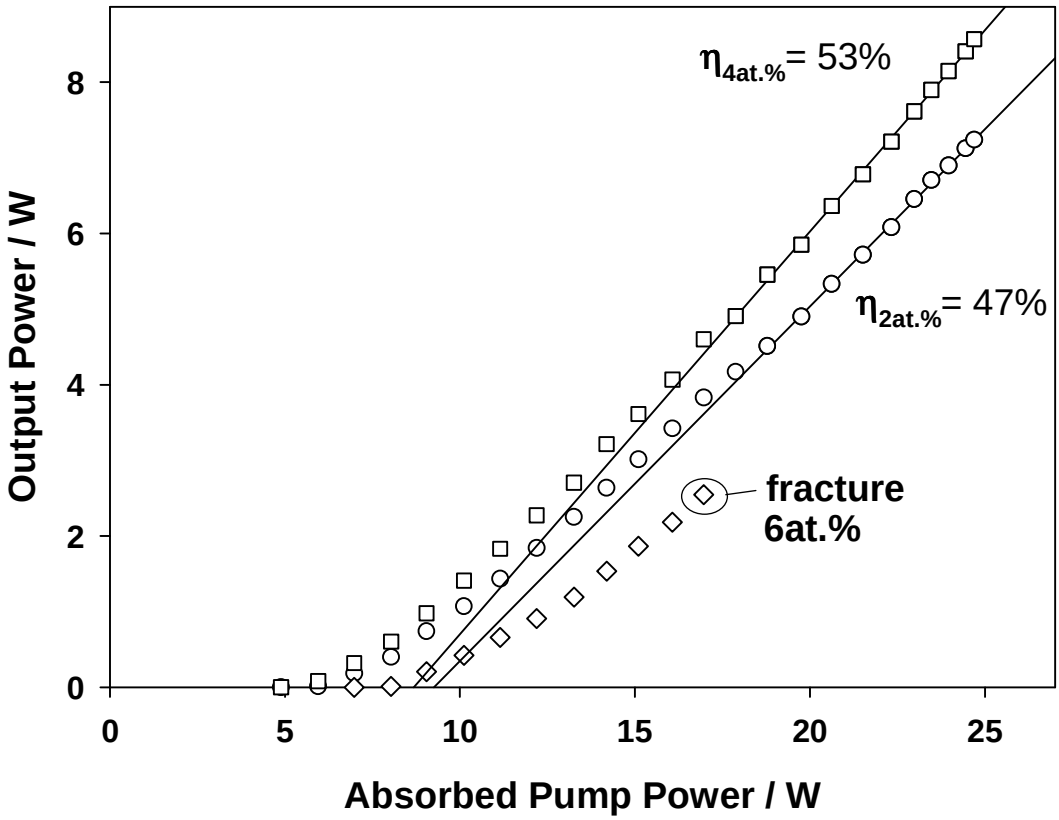
η4at.%= 53%
η2at.%= 47%
fracture
6at.%
Output Power / W
Absorbed Pump Power / W
0
2
4
6
8
0
5
10
15
20
25

Figure 3

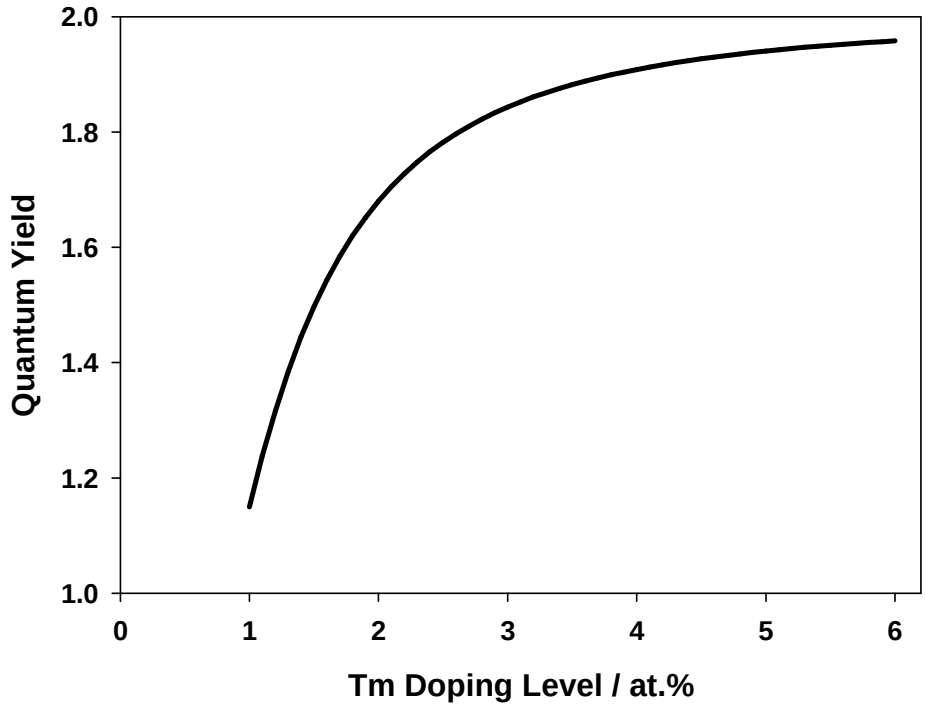

Figure 4

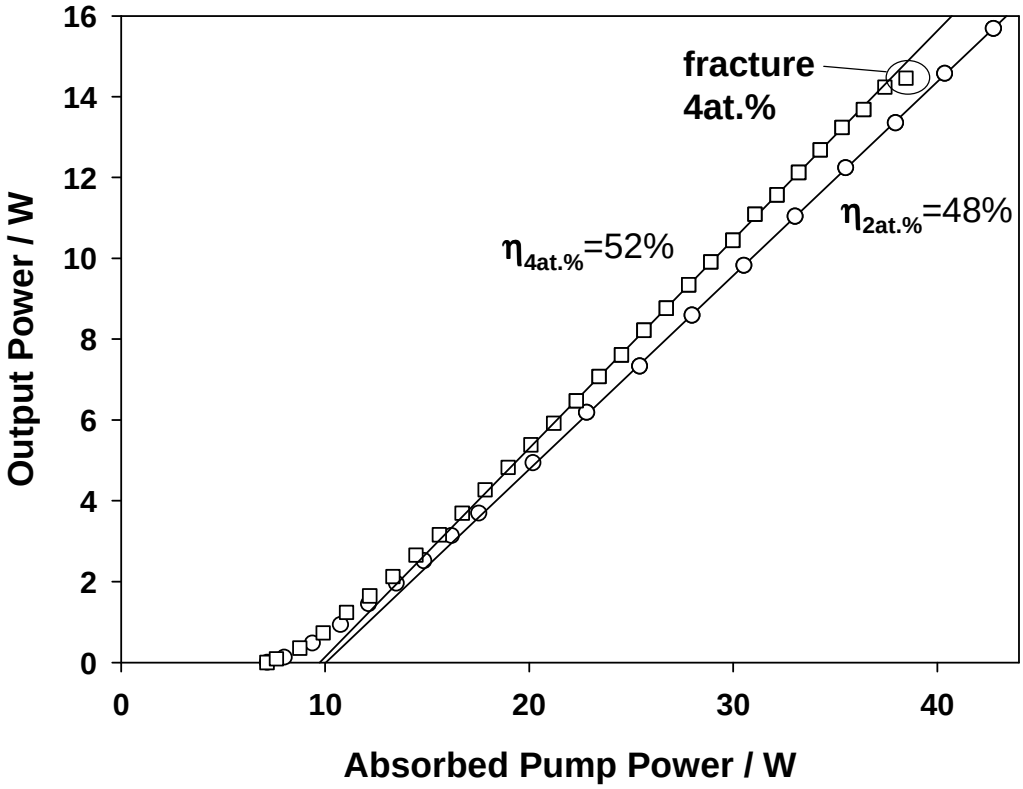
fracture
4at.%
η4at.%=52%
η2at.%=48%
Output Power / W
Absorbed Pump Power / W
0
2
4
6
8
10
12
14
16
0
10
20
30
40

Figure 5

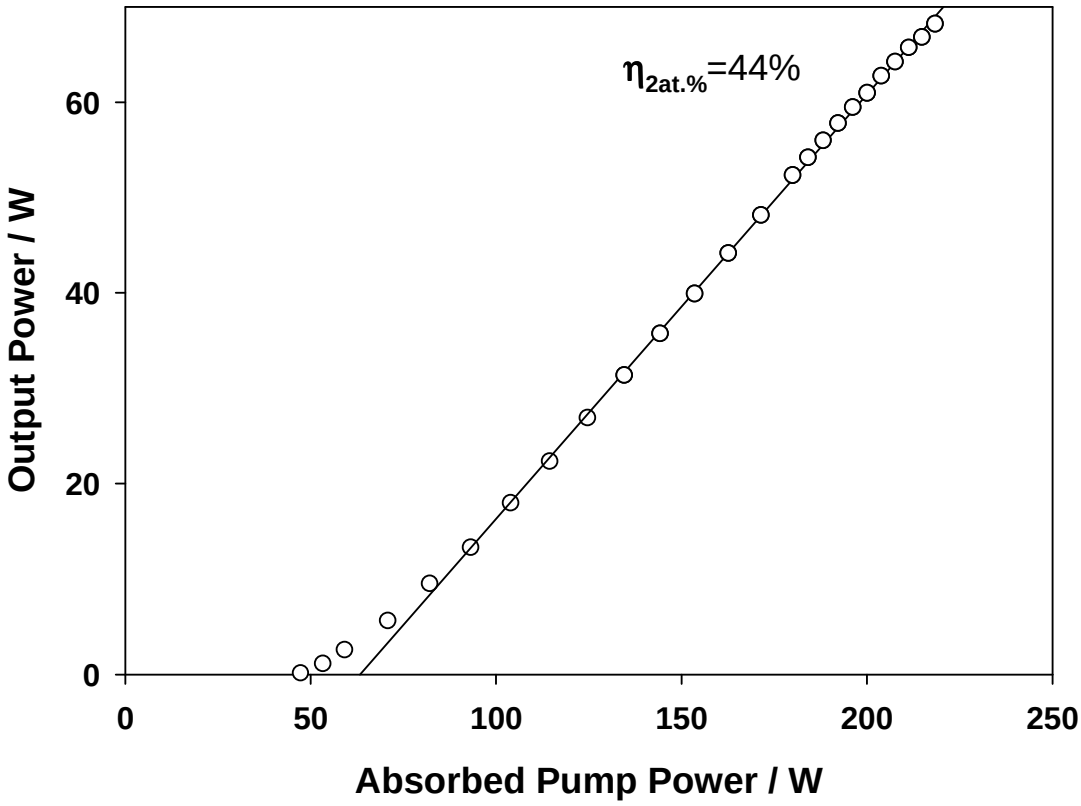
$\eta_{2at.\%}$=44%
Output Power / W
0
20
40
60
0
50
100
150
200
250
Absorbed Pump Power / W